Journal of Nuclear Medicine, published on April 23, 2021 as doi:10.2967/jnumed.121.262283

Machine-learning with ^{18}F-sodium fluoride PET and quantitative plaque analysis on CT angiography for the future risk of myocardial infarction

Jacek Kwiecinski[a,b], Evangelos Tzolos [a,c], Mohammed N Meah[c], Sebastien Cadet[a], Philip D Adamson[d], Kajetan Grodecki[a], Nikhil V Joshi [e], Alastair J Moss[c], Michelle C Williams[c], Edwin JR van Beek MD, PhD [c,f], Daniel S Berman[a], David E Newby[c], Damini Dey[a], Marc R Dweck[c], Piotr J Slomka[a]

[a] Department of Imaging (Division of Nuclear Medicine), Medicine (Division of Artificial Intelligence in Medicine), and Biomedical Sciences, Cedars-Sinai Medical Center, Los Angeles, CA, USA
[b] Department of Interventional Cardiology and Angiology, Institute of Cardiology, Warsaw, Poland
[c] BHF Centre for Cardiovascular Science, University of Edinburgh, Edinburgh, United Kingdom
[d] Christchurch Heart Institute, University of Otago, Christchurch, New Zealand
[e] Bristol Heart Institute, University of Bristol, United Kingdom
[f] Edinburgh Imaging, Queens Medical Research Institute, University of Edinburgh, Edinburgh, United Kingdom

Brief Title: AI for coronary PET and CT angiography

Address for Correspondence:

Piotr J. Slomka, PhD
Cedars-Sinai Medical Center
8700 Beverly Blvd, Metro 203
Los Angeles, CA 90048, USA
Email: piotr.slomka@cshs.org
Phone: 310-423-4348 Fax: 310-423-0173
Twitter: @Piotr_JSlomka
https://orcid.org/0000-0002-6110-938X

Funding and Acknowledgements

This research was supported in part by grants R01HL135557 and R01HL133616 from the National Heart, Lung, and Blood Institute/National Institute of Health (NHLBI/NIH). The content is solely the responsibility of the authors and does not necessarily represent the official views of the National Institutes of Health.

DEN (CH/09/002, RE/18/5/34216, RG/16/10/32375), MRD (FS/14/78/31020), MM (FS/19/46/34445) and MCW (FS/11/014, CH/09/002, FS/ICRF/20/26002) are supported by the British Heart Foundation. PDA is supported by Heart Foundation of New Zealand Senior Fellowship (1844). ET was supported by a grant from Dr. Miriam and Sheldon G. Adelson Medical Research Foundation. DEN is the recipient of a Wellcome Trust Senior Investigator Award (WT103782AIA) and MRD of the Sir Jules Thorn Award for Biomedical Research Award (2015). EJRVB is supported by SINAPSE (Scottish Imaging Network – A Platform of Scientific Excellence). NVJ is supported by the Medical Research Council through MRC Clinical Academic Research Partnership grant (MR/T005459/1).

Disclosures

The authors declare that they have no relevant or material financial interests that relate to the research described in this paper.

Word count: 4982

Abstract

Coronary ^{18}F-sodium fluoride (^{18}F-NaF) positron emission tomography (PET) and computed tomography (CT) angiography-based quantitative plaque analysis have shown promise in refining risk stratification in patients with coronary artery disease. We combined both of these novel imaging approaches to develop an optimal machine-learning model for the future risk of myocardial infarction in patients with stable coronary disease.

Methods

Patients with known coronary artery disease underwent coronary ^{18}F-NaF PET and CT angiography on a hybrid PET/CT scanner. Machine-learning by extreme gradient boosting was trained using clinical data, CT quantitative plaque analysis measures and ^{18}F-NaF PET, and it was tested using repeated 10-fold hold-out testing.

Results

Among 293 study participants (65±9 years; 84% male), 22 subjects experienced a myocardial infarction over the 53 [40-59] months of follow-up. On univariable receiver-operator-curve analysis, only ^{18}F-NaF coronary uptake emerged as a predictor of myocardial infarction (c-statistic 0.76, 95% confidence interval [CI] 0.68-0.83). When incorporated into machine-learning models, clinical characteristics showed limited predictive performance (c-statistic 0.64, 95% CI 0.53-0.76;) and were outperformed by a quantitative plaque analysis-based machine-learning model (c-statistic 0.72, 95% CI 0.60-0.84). After inclusion of all available data (clinical, quantitative plaque and ^{18}F-NaF PET), we achieved a substantial improvement (p=0.008 versus ^{18}F-NaF PET alone) in the model performance (c-statistic 0.85, 95% CI 0.79-0.91).

Conclusions

Both ^{18}F-NaF uptake and quantitative plaque analysis measures are additive and strong predictors of outcome in patients with established coronary artery disease. Optimal risk stratification can be achieved by combining clinical data with these approaches in a machine-learning model.

Keywords: myocardial infarction, computed tomography, ^{18}F-NaF positron emission tomography, quantitative plaque analysis, machine-learning

Introduction

In every day clinical practice, prediction of myocardial infarction is challenging and is typically based on cardiovascular risk factors and scores, especially in subjects with suspected coronary artery disease (1). However, in patients with established coronary artery disease, the performance of risk scores is limited with c-statics ranging from 0.60 to 0.68 (1). Recently, advanced imaging techniques have demonstrated considerable promise in refining risk stratification in patients with established coronary artery disease. We have demonstrated that assessment of disease activity in the coronary arteries with ^{18}F-sodium fluoride (^{18}F-NaF) positron emission tomography (PET) outperforms clinical variables and risk scores for the prediction of myocardial infarction in patients with a high burden of coronary artery disease (2,3). Similarly, in observational studies and a sub-analysis of the SCOT-HEART trial, quantitative plaque analysis investigating both plaque type and burden on contrast enhanced CT angiography has emerged as a major predictor of adverse outcomes (4,5). To date, no study has investigated whether these two promising methods (which can be obtained during a single imaging session on a hybrid PET/CT scanner) are interchangeable or can provide superior predictive performance when used in combination.

In this study, we employed machine-learning to investigate whether the prognostic information provided by quantitative CT plaque analysis and assessments of disease activity by ^{18}F-NaF PET are complementary, and to develop an optimized model to determine the future risk of myocardial infarction in patients with established coronary artery disease (6).

Methods

Study population

The current study is based on a cohort of patients with established coronary artery disease on guideline recommended medical treatments which we assembled for our previous publication regarding the prognostic utility of ^{18}F-NaF PET (2). However, in the current study, we have included longer follow-up and utilized novel quantitative plaque analysis of coronary CT angiography. Our work is focused specifically upon whether machine learning methods can combine the prognostic information provided by clinical factors, quantitative CT plaque analysis and ^{18}F-NaF PET to improve the prediction of myocardial infarction. All participants underwent hybrid coronary ^{18}F-NaF PET and contrast CT coronary angiography within prospective observational research studies (NCT01749254, NCT02110303, NCT02607748) (3,7,8). All patients had established coronary artery disease and underwent a comprehensive baseline clinical assessment with evaluation of their cardiovascular risk factor profile including calculation of the Secondary Manifestations of ARTerial disease (SMART) risk score (Supplementary Material) (1). Studies were conducted with the approval of the local research ethics committee, in accordance with the Declaration of Helsinki, and with written informed consent from each participant.

CT Angiography and ^{18}F-Sodium Fluoride PET

Acquisition and Reconstruction

Patients underwent ^{18}F-NaF PET on hybrid PET/CT scanners (128-slice Biograph mCT, Siemens Medical Systems, Knoxville, USA or Discovery 710 GE Healthcare, Milwaukee, WI, USA) 60 min following intravenous administration of ^{18}F-NaF (250 MBq). We acquired a non-contrast CT

attenuation correction scan followed by a 30-min PET emission scan in list mode, a low-dose non-contrast ECG-gated CT for calculation of the coronary calcium and a contrast-enhanced ECG-gated coronary CT angiogram (CTA) which was obtained in mid-diastole and end-expiration on the same PET/CT system without repositioning the patient. The ECG-gated PET list mode dataset was reconstructed using harmonized protocols as described previously (supplementary material) (8-10).

Coronary microcalcification activity (CMA) quantification

Image analysis was performed in FusionQuant (Cedars-Sinai Medical Center, Los Angeles) (11). We used a recently described measure of coronary ^{18}F-NaF uptake, coronary microcalcification activity (CMA) that quantifies PET activity across the entire coronary vasculature (12). CMA is a highly reproducible and robust measure of disease activity predicting both disease progression and myocardial infarction (2, 13). We calculated the per vessel and per patient CMA (Figure 1), maximum coronary SUV and target to background ratio (TBR) as described previously (supplementary material) (3, 12).

Computed Tomography

The coronary artery calcium score was measured in Agatston units (AU) using clinical software (NetraMD, ScImage, Los Altos, CA, USA) on non-contrast CT scans. The presence, extent and severity of coronary artery disease were evaluated on contrast-enhanced CT angiography by defining the segment involvement score, DUKE coronary artery disease index and the number of vessels with >50% luminal stenosis (14). Multivessel coronary artery disease was defined as at least 2 major epicardial vessels with any combination of either >50% stenosis, or previous revascularization.

Quantitative Plaque Analysis of CT angiography

We performed quantitative plaque analysis of all coronary segments with a lumen diameter greater than 2 mm using semi-automated software (AutoPlaque version 2.0, Cedars-Sinai Medical Center, Los Angeles, USA) (4,5). Proximal and distal limits of lesions were manually marked by an experienced reader after examination of coronary CT angiography images in multiplanar format. Subsequent plaque quantification was fully automated using adaptive scan-specific thresholds. Total, calcified, non-calcified as well as low attenuation plaque volumes were calculated. The plaque burden was calculated according to the following equation (plaque volume x 100%/vessel volume). The contrast density difference was the maximal difference in contrast density (mean Hounsfield unit / cross-sectional area) in the plaque and the reference proximal vessel cross section.

Machine-learning

Machine learning was used to derive a joint score for myocardial infarction by incorporating the key clinical variables, quantitative CT variables, and ^{18}F-NaF PET findings.

Model Building

XGBoost is a recent implementation of a gradient boosting algorithm, which iteratively trains a set of weak learners (simple decision trees) using a given set of patient data, to build a combined strong classifier to identify an outcome (15). For every patient, the XGBoost algorithm computes an individualized probability of outcome, considering all input variables.

We applied XGBoost for prediction of myocardial infarction by building 3 models. First, a clinical model with baseline clinical characteristics: age, gender, co-morbidities, medication, biomarkers, past medical history and coronary calcium score (model 1). The second model was

derived from quantitative plaque analysis variables (including low attenuation plaque burden and the contrast density difference). A final model incorporated clinical, CT and ^{18}F-NaF PET data in combination. All variables utilized in the machine-learning modelling are presented in Supplementary Table 1.

Model Testing

Given the limited number of cases, we refrained from performing data-specific hypertuning and applied fixed XGBoost parameters established in our previous studies (15). Furthermore, to avoid biased results and limit overfitting, we tested all of our models using repeated 10-fold cross-testing, which separates training and testing data (16). The dataset was randomly split into 10 folds with similar myocardial infarction rates in each fold (stratified 10 folds). Ten models were created each from 90% of the data, and each tested in held-out test sample (10% of the data). These 10 held-out samples containing non-overlapping test results were subsequently concatenated to evaluate the average performance of XGBoost in unseen data.

Feature importance

To elucidate the influence of each of the variables included in the machine-learning model, we provided machine-learning feature importance scores. Importance is the relative amount that each attribute improves the XGBoost performance measure. The variable importance was determined directly from the xgboost model separately in each fold and returned from the XGBoost model for each variable. The variable importance represents the relative improvement in the log loss objective function of the xgboost (17).

Clinical follow-up

The primary endpoint of the study was fatal or non-fatal myocardial infarction. Outcome information was obtained in June 2020 from the local and national healthcare record systems that integrates primary and secondary health care records. Categorization of these outcomes was performed blinded to the coronary CT angiography and PET data.

Statistical analysis

We assessed the distribution of data with the Shapiro-Wilk test. Continuous parametric variables were expressed as mean ± standard deviation, and non-parametric data were presented as median [interquartile interval]. Fisher's exact test or chi-squared test was used for analysis of categorical variables. The performance of machine-learning models and single clinical characteristics in predicting myocardial infarction was assessed using receiver operator characteristic (ROC) analysis, and the area under the curve (c-statistic) values were compared with the DeLong test (18). Statistical analysis was performed with SPSS version 24 (IBM SPSS Statistics for Windows, Version 24.0. Armonk, NY: IBM Corp) and R studio and R software version 4.01 (R Foundation for Statistical Computing, Vienna, Austria). A two-sided $p<0.05$ was considered statistically significant.

Results

All 293 study participants (65±9 years; 84% male) had established coronary artery disease and were on guideline recommended medical treatments (Table 1). Two-hundred and thirty-seven (81%) patients had a history of revascularization, 191 (65%) had multi-vessel obstructive coronary artery disease and the median coronary calcium score was 334 [76 to 804] AU. Over the 53 [40-59] months of follow-up, 22 subjects experienced a fatal (n=3) or non-fatal (n=19) myocardial infarction.

The high burden of atherosclerosis was reflected in the quantitative plaque analysis derived from coronary CT angiography. The median total plaque volume was 1174 [716 to 1772] mm^3 and consisted largely of non-calcified plaque (1099 [647 to 1574] mm^3) with a substantial volume of low-attenuation plaque (88 [44 to 167] mm^3). Over half of the study population (166 [56%]) had a low-attenuation plaque burden exceeding 4%. On PET, 109 (37.2%) patients presented with a high ^{18}F-NaF coronary microcalcification activity (CMA>1.56; Figure 2).

On receiver operator curve analysis, ^{18}F-NaF CMA (c-statistic 0.76, 95% confidence interval (CI) 0.68 to 0.83; p<0.001), maximum ^{18}F-NaF TBR (c-statistic 0.72, 95% CI 0.63 to 0.82; p<0.001) and maximum ^{18}F-NaF SUV (c-statistic 0.70, 95% CI 0.59 to 0.81; p=0.002) were the only statistically significant predictors of myocardial infarction. In contrast, baseline clinical characteristics, luminal stenosis severity, qualitative or quantitative CT-derived variables were not significant predictors of myocardial infarction on their own (Table 2). However, when incorporated into machine-learning models, the aforementioned variables emerged as predictors of adverse events. While a model based on clinical characteristics only showed limited predictive performance with a c-statistic of 0.64 (95% CI 0.53-0.76), the quantitative plaque analysis-based

machine-learning model outperformed the former with a c-statistic of 0.72 (95% CI 0.60-0.84, p=0.02) which was comparable to ^{18}F-NaF CMA alone (p=0.47). Inclusion of clinical data improved the ^{18}F-NaF CMA and quantitative plaque analysis-based models only slightly (0.77 [95% CI 0.69-0.84] and 0.74 [95% CI 0.64-0.83] respectively). Importantly, after inclusion of all available data (clinical, quantitative plaque and ^{18}F-NaF PET), we achieved an increase in model performance with a c-statistic of 0.85 (95% CI 0.79-0.91, p<0.001) which was higher than the quantitative CT plaque model (p=0.008) and the ^{18}F-NaF CMA (p=0.01; Figures 3 and 4) as well as the clinical characteristics model (p<0.001).

Discussion

We have built a machine-learning model for risk stratification in patients with established coronary artery disease. In our cohort of patients with advanced coronary atherosclerosis, we showed that risk prediction does not depend on cardiovascular risk scores, stenosis severity or CT calcium scoring. Rather the risk of myocardial infarction is primarily governed by the analysis of plaque type and plaque burden provided by coronary CT angiography and assessments of disease activity by ^{18}F-NaF PET. Importantly, our machine learning approach has overcome the challenges posed by co-linearity of these variables and, for the first time, has demonstrated that this information is complementary and additive with the combination of both providing the most robust outcome prediction. If confirmed in further studies this comprehensive approach holds major promise in refining risk stratification of patients with established coronary artery disease, a population where such prediction is currently challenging. Importantly, such stratification in these patients can be achieved objectively with quantitative variables obtained on a single hybrid PET/CT acquisition.

^{18}F-NaF PET provides an assessment of vascular injury and disease activity across a wide spectrum of cardiovascular conditions including aortic stenosis, mitral annular calcification, abdominal aortic aneurysm, erectile dysfunction, bioprosthetic valve degeneration and coronary artery disease (2, 19-21). Indeed, baseline ^{18}F-NaF PET is consistently associated with future disease progression and adverse events in each of these conditions. On the other hand, quantitative assessment of atherosclerotic plaque on contrast-enhanced CT angiography allows us to measure the burden of different types of plaque across the coronary arteries (4). We recently demonstrated that the low-attenuation plaque burden provides powerful prediction of

myocardial infarction, outperforming cardiovascular risk scores, Agatston coronary artery calcium scoring, or the presence and severity of obstructive coronary artery disease. Whether these two exciting developments can be used in combination to further advance risk prediction was previously unknown.

Using the information from these approaches and by leveraging machine-learning, we were able to build an integrated model for prediction of events in patients with established coronary artery disease, a group of patients where risk prediction is currently challenging. The XGBoost algorithm has been successfully implemented for risk prediction in a wide range of clinical scenarios (15, 22). It enables the incorporation of numerous predictors into the model even when these variables are correlated - a major limitation with conventional regression analyses. While we have previously shown that ^{18}F-NaF uptake is associated with quantitative plaque analysis indices, our current analysis highlights the complementary prognostic information that PET and quantitative CT plaque assessments provide together (23, 24). Indeed, our machine learning model incorporating the information from these two modalities alongside clinical factors outperformed the individual components analyzed separately with a high c-statistic of 0.85. Importantly, our study also underscores that in patients with advanced coronary artery disease, markers of disease activity, plaque type and plaque burden provide superior risk prediction to clinical risk scores and conventional coronary calcium CT analyses.

According to societal guidelines, patients with clinically manifest atherosclerotic arterial disease are considered to be at very high risk of a recurrent cardiovascular events and cardiovascular mortality. However, in everyday clinical practice, it is apparent that there is a wide distribution of actual risk for recurrent vascular events in patients with clinically established arterial disease. While the population of subjects with manifested coronary artery disease is rapidly growing,

accurate risk prediction in this important population remains challenging. The guideline recommended SMART risk score was shown to have only a moderate c-statistic (0.64-0.68), and there is a paucity of data regarding the role imaging could play in this cohort (1). In our study we have targeted this important high-risk population. We have demonstrated that quantitative plaque analysis measures and the coronary microcalcification activity considerably improve stratification of patients' risk (c-statistic 0.85). In a conservative 10-fold cross testing machine learning model, we showed that CT and PET data need to be employed together for optimal stratification.

Limitations

With the limited number of patients and events, our findings require confirmation in future studies. Machine-learning models can perform better when trained within bigger datasets and therefore further studies are needed to confirm our findings and allow further testing to refine and to calibrate the machine-learning models. External validation of our findings in other cohorts is needed. While this is currently challenging given that ^{18}F-NaF PET is an emerging technique, this will be possible in the future using outcome data from the Prediction of Recurrent Events With ^{18}F-Fluoride (PREFFIR) study which is prospectively investigating the ability of ^{18}F-NaF coronary PET and CT angiography to predict recurrent events in patients with multi-vessel disease and recent myocardial infarction. Since the majority of study participants had multivessel disease future studies should characterize the utility of ^{18}F-NaF PET in single vessel disease patients.

In conclusion, both ^{18}F-NaF uptake and quantitative plaque analysis measures from contrast CT are strong predictors of outcome in patients with established coronary artery disease. Optimal risk stratification can be achieved by combining these imaging assessments of plaque type, burden and activity with clinical variables in a machine-learning model.

Key Points:

Question: Does combining information provided by CT plaque analysis and assessments of disease activity by 18F-NaF PET with machine-learning enhance risk stratification in established coronary artery disease?

Pertinent Findings: In a post hoc analysis of data collected for prospective observational studies, on a cohort of 293 patients with established coronary artery disease, we have demonstrated that optimal risk stratification can be achieved by combining clinical data with 18F-sodium fluoride PET and quantitative coronary CT angiography plaque analysis in a machine-learning model.

Implications for Patient Care: This approach has major potential for the risk stratification of patients with established coronary artery disease.

References

1. Dorresteijn JA, Visseren FL, Wassink AM, et al. Development and validation of a prediction rule for recurrent vascular events based on a cohort study of patients with arterial disease:the SMART risk score. Heart 2013;99:866-72.
2. Kwiecinski J, Tzolos E, Adamson PD, et al. 18F-Sodium Fluoride Coronary Uptake Predicts Outcome in Patients with Coronary Artery Disease. J Am Coll Cardiol 2020;75:3061-74
3. Joshi NV, Vesey AT, Williams MC, et al. 18F-fluoride positron emission tomography for identification of ruptured and high-risk coronary atherosclerotic plaques: a prospective clinical trial. Lancet 2014;383:705-13.
4. Hell MM, Motwani M, Otaki Y, et al. Quantitative global plaque characteristics from coronary computed tomography angiography for the prediction of future cardiac mortality during long-term follow-up. Eur Heart J Cardiovasc Imaging 2017;18:1331-1339.
5. Williams M, Kwiecinski J, Doris M, et al. Low attenuation noncalcified plaque on coronary computed tomography angiography predicts myocardial infarction. Circulation 2020;(18),1452-1462 DOI:10.1161/CIRCULATIONAHA.119.044720.
6. Motwani M, Dey D, Berman DS, Germano G, et al. Machine-learning for prediction of all-cause mortality in patients with suspected coronary artery disease: a 5-year multicentreprospective registry analysis. Eur Heart J 2016;38:500–507.
7. Moss AJ, Dweck MR, Doris MK, et al. Ticagrelor to reduce myocardial injury in patients with high-risk coronary artery plaque. J Am Coll Cardiol Img 2020;13(7):1549-1560

8. Doris MK, Otaki Y, Krishnan SK, et al. Optimization of reconstruction and quantification of motion-corrected coronary PET-CT. J Nucl Cardiol 2020;27(2):494-504. doi: 10.1007/s12350-018-1317-5
9. Rubeaux M, Joshi N, Dweck MR, et al. Motion correction of 18F-sodium fluoride PET for imaging coronary atherosclerotic plaques. J Nucl Med 2016;57:54-9
10. Lassen ML, Kwiecinski J, Dey D, et al. . Triple-gated motion and blood pool clearance corrections improve reproducibility of coronary 18F-NaF PET. Eur J Nucl Med Mol Imaging. 2019;46:2610–2620
11. Massera D, Doris MK, Cadet S, et al. Analytical quantification of aortic valve 18F-sodium fluoride PET uptake. J Nucl Cardiol. 2020 27(3):962-972. doi: 10.1007/s12350-018-01542-6.
12. Kwiecinski J, Cadet S, Daghem M, et al. Whole-vessel coronary 18F-sodium fluoride PET for assessment of the global coronary microcalcification burden. Eur J Nucl Med Mol Imaging. 2020;47:1736–1745
13. Tzolos E, Kwiecinski J, Lassen ML, et al. Observer repeatability and interscan reproducibility of 18F-sodium fluoride coronary microcalcification activity. J. Nucl. Cardiol. (2020). https://doi.org/10.1007/s12350-020-02221-1
14. Leipsic J, Abbara S, Achenbach S, et al. SCCT guidelines for the interpretation and reporting of coronary CT angiography: a report of the Society of Cardiovascular Computed Tomography Guidelines Committee. J Cardiovasc Comput Tomogr 2014;8:342–58

15. Commandeur F, Slomka PJ, Goeller M, et al. Machine-learning to predict the long-term risk of myocardial infarction and cardiac death based on clinical risk, coronary calcium, and epicardial adipose tissue: a prospective study. Cardiovasc Res 2019 Dec 19:cvz321.
16. Kim J-H. Estimating classification error rate: Repeated cross-validation, repeated hold-out and bootstrap. Comput Stat Data Anal 2009;53:3735-3745.
17. Hastie T, Tibshirani R, Friedman J. The Elements of Statistical Learning Data Mining, Inference and Prediction. Springer 2001; page: 367
18. DeLong ER, DeLong DM, Clarke-Pearson DL. Comparing the areas under two or more correlated receiver operating characteristic curves: a nonparametric approach. Biometrics 1988;44:837-45
19. Dweck MR, Jenkins WSA, Vesey AT, et al. 18F-Sodium Fluoride Uptake Is a Marker of Active Calcification and Disease Progression in Patients With Aortic Stenosis. Circulation-Cardiovascular Imaging. 2014;7(2),371-378.
20. Cartlidge TRG, Doris MK, Sellers SL, et al. Detection and prediction of bioprosthetic aortic valve degeneration. J Am Coll Cardiol 2019;73:1107–19.
21. Forsythe RO, Dweck MR, McBride OMB, et al. F-18-Sodium Fluoride Uptake in Abdominal Aortic Aneurysms The SoFIA(3) Study. Journal of the American College of Cardiology, 71(5), 513-523.
22. van Rosendael AR, Maliakal G, Kolli KK, et al. Maximization of the usage of coronary CTA derived plaque information using a machine-learning based algorithm to improve risk stratification; insights from the CONFIRM registry. J Cardiovasc Comput Tomogr 2018;12:204–209.

23. Kwiecinski J, Dey D, Cadet S, et al. Predictors of 18F-sodium fluoride uptake in patients with stable coronary artery disease and adverse plaque features on computed tomography angiography. Eur Heart J Cardiovasc Imaging 2020 21(1):58-66. doi: 10.1093/ehjci/jez152

24. Kwiecinski J, Dey D, Cadet S, et al. Peri-coronary adipose tissue density is associated with 18F-sodium fluoride coronary uptake in stable patients with high-risk plaques. JACC Cardiovasc Imaging. 2019;12:2000–10.

Tables

Table 1. Baseline clinical characteristics.

Category	Variable	Mean±sd/median[Q1-Q3]/n (%)
Baseline Clinical Characteristics	Age	65±9
	Men	245 (84%)
	Body-mass index (kg/m^2),	29±5
	Systolic blood pressure (mm Hg)	141±20
	Diastolic blood pressure (mm Hg)	79±11
Cardiovascular history	History of acute coronary syndrome	161 (55.1%)
	History of percutaneous coronary intervention	182 (62.3%)
	History of coronary artery bypass graft surgery	48 (16.4%)
	History of angina	136 (46.6%)
	Recent acute coronary syndrome	61 (21%)
	Cerebrovascular accident or transient ischemic attack	9 (3.1%)
Comorbidities/risk factors	Hypertension	174 (59.6%)

	Hyperlipidemia	257 (88%)
	Diabetes mellitus	61 (20.8%)
	Current smoking Ex-smoker	58 (19.9%) 137 (46.9%)
	Atrial fibrillation	10 (3.4%)
	Peripheral vascular disease	16 (5.5%)
Medications *	Aspirin	268 (91.8%)
	Dual antiplatelet therapy	62 (21.2%)
	Statin	262 (89.7%)
	Beta Blocker	196 (67.1%)
	Angiotensin-converting enzyme inhibitor or angiotensin receptor blocker	197 (67.4%)
	Insulin	4 (1.4 %)
	Oral diabetic medications	48 (16.4%)
	Calcium blockers	63 (21.6%)
	Diuretics	38 (16.0%)
Biomarkers	Total cholesterol (mg/dL)	159 [139-182]

	LDL cholesterol (mg/dL)	73 [46-93]
	HDL cholesterol (mg/dL)	46 [39-66]
	Triglycerides (mg/dL)	133 [97-204]
	Creatinine (mg/dL)	0.9 [0.8-1.0]
Risk Scores	SMART	18 [13-26]
Computed Tomography – qualitative & non-contrast	- Single vessel disease - Two vessel disease - Three vessel disease - Left main stem involvement	87 (29.8%) 110 (37.7%) 81 (27.6%) 18 (6.1%)
	Coronary stent	218 (73.4%)
	Segment involvement score	5 [3-7]
	Segment involvement score >5	145 (73.5%)
	Coronary calcium score	334 [76-804]
	Coronary calcium score category 0-99 100-399 400-999 >1000	 84 (28.7%) 76 (25.9%) 74 (25.3%) 59 (20.1%)

Computed tomography - quantitative	Total plaque volume, mm^3	1174 [716, 1772]
	Non-calcified plaque volume, mm^3	1099 [647, 1574]
	Calcified plaque volume, mm^3	77 [23, 180]
	Low-attenuation plaque volume, mm^3	88 [44, 167]
	Total plaque burden, %	55 [49, 63]
	Non-calcified plaque burden, %	51 [45, 57]
	Calcified plaque burden, %	3.5 [1.4, 7.9]
	Low-attenuation plaque burden, %	4.4 [2.6, 7.0]
	Area stenosis, %	58 [47, 75]
	Contrast density difference, %	29 [24, 37]
	Ischemia score	31 [21, 47]
^{18}F-NaF PET	CMA	0.66 [0-2.84]
	TBRmax	1.22 [1.1-1.42]
	SUVmax	1.44 [1.19, 1.71]
Outcome	Myocardial infarction	22 (7.5%)

CMA – coronary microcalcification activity, PET – positron emission tomography, ^{18}F-NaF – ^{18}F-sodium fluoride, SMART - Secondary Manifestations of ARTerial disease risk score, SUVmax – maximum standard uptake value, TBRmax – maximum target to background ratio

Recent acute coronary syndrome was defined as an event within less than 14 days prior to PET imaging.

Table 2. Prediction of myocardial infarction in patients with advanced coronary artery disease. Receiver operator curve modelling for prediction of myocardial infarction.

Category	Variable	Area under the curve (95% confidence intervals)	p value
Baseline Clinical Characteristics	Age	0.51 (0.35-0.67)	0.81
	Sex	0.51 (0.38-0.64)	0.84
	Body-mass index	0.58 (0.46-0.70)	0.23
	Systolic blood pressure	0.52 (0.37-0.67)	0.74
Past Medical History	Myocardial infarction	0.45 (0.33-0.58)	0.48
	Recent acute coronary syndrome	0.57 (0.43-0.71)	0.33
	Percutaneous coronary intervention	0.53 (0.40-0.67)	0.66
	Coronary artery bypass graft	0.52 (0.39-0.65)	0.80
	Cerebrovascular accident	0.53 (0.40-0.67)	0.60
Comorbidities	Hypertension	0.47 (0.35-0.59)	0.57
	Hyperlipidaemia	0.48 (0.35-0.60)	0.61
	Diabetes	0.51 (0.37-0.65)	0.29
	Smoking	0.46 (0.32-0.60)	0.59
	Peripheral vascular disease	0.52 (0.39-0.66)	0.80
Biomarkers	Total cholesterol (mmol/L)	0.53 (0.38-0.68)	0.68
	LDL cholesterol (mmol/L)	0.59 (0.43-0.75)	0.18

	HDL cholesterol (mmol/L)	0.53 (0.38-0.67)	0.71
	Triglycerides (mmol/L)	0.57 (0.44-0.69)	0.33
	Creatinine (μmol/L)	0.54 (0.40-0.68)	0.54
Risk scores	SMART	0.57 (0.43-0.70)	0.35
Computed Tomography – qualitative & non-contrast	Multivessel disease	0.55 (0.42-0.68)	0.48
	Segment involvement score	0.56 (0.41-0.71)	0.40
	Coronary calcium score	0.51 (0.37-0.66)	0.87
	Modified Duke index	0.61 (0.48-0.74)	0.11
Computed tomography - quantitative	Total plaque volume	0.53 (0.39-0.67)	0.65
	Non-calcified plaque volume	0.54 (0.40-0.68)	0.53
	Calcified plaque volume	0.46 (0.33-0.58)	0.48
	Low-attenuation plaque volume	0.57 (0.41-0.72)	0.30
	Total plaque burden	0.45 (0.33-0.57)	0.42
	Non-calcified plaque burden	0.47 (0.35-0.59)	0.67
	Calcified plaque burden	0.41 (0.29-0.54)	0.16
	Low-attenuation plaque burden	0.61 (0.48-0.75)	0.071
	Area stenosis	0.48 (0.35-0.62)	0.79
	Contrast density difference	0.56 (0.40-0.71)	0.33
	Ischemia score	0.52 (0.38-0.65)	0.77
^{18}F-NaF PET	CMA total	0.76 (0.68-0.83)	<0.001
	TBRmax	0.72 (0.63-0.82)	<0.001
	SUVmax	0.70 (0.59-0.81)	0.002

CMA – coronary microcalcification activity, HDL – High density lipoprotein, LDL – low density lipoprotein, SD – standard deviation, PET – positron emission tomography, ^{18}F-NaF – ^{18}F-sodium fluoride, SMART - Secondary Manifestations of ARTerial disease risk score, SUVmax – maximum standard uptake value, TBRmax – maximum target to background ratio.

Figures

Figure 1. Measuring Disease Activity Across the Coronary Vasculature with ^{18}F-NaF Coronary Microcalcification Activity (CMA) and the Low Attenuation Plaque Burden with Quantitative Plaque Analysis. 3-Dimensional rendering of coronary CT angiography co-registered with PET for evaluation of ^{18}F-sodium fluoride uptake (blue and red; left panel). The coronary microcalcification activity (CMA) is a summary measure of ^{18}F-NaF activity across the entire coronary vasculature as it includes all counts originating from the coronary arteries 3-Dimensional rendering of CT angiography based quantitative plaque analysis with orange low attenuation plaque (LAP) and yellow calcified plaque. The low attenuation plaque burden was defined as the LAP volume x 100%/vessel volume.

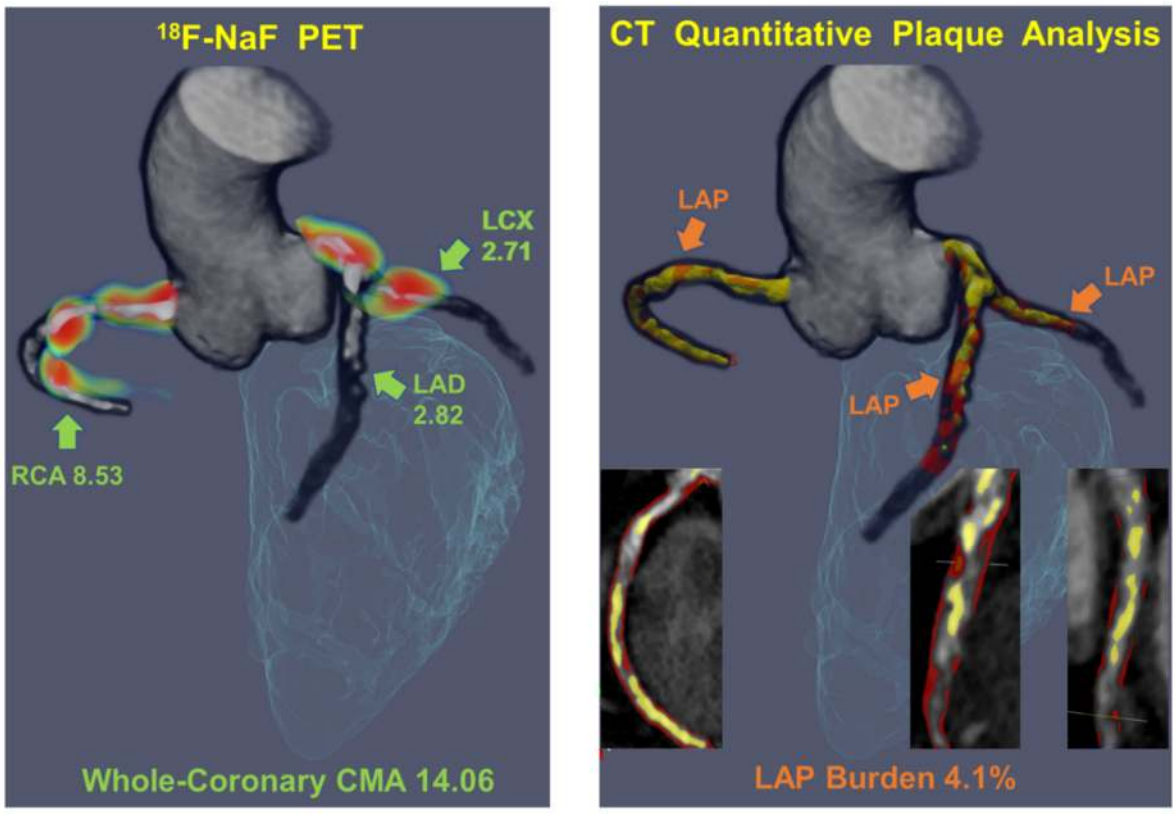

LAD – left anterior descending, LCX – left circumflex, RCA – Right coronary artery

Figure 2. Case examples of quantitative plaque analysis on coronary CT angiography and ^{18}F-sodium fluoride positron emission tomography in patients with established coronary artery disease. Hybrid CT angiography and ^{18}F-NaF positron emission tomography of coronary arteries in: (A) a 70-year-old male who presented with diffused largely non-calcified disease (middle panel in red) in the LAD and demonstrated increased ^{18}F-NaF uptake in the LAD on positron emission tomography. (B) a 59-year-old male with mild LCX atherosclerosis, who presented with a high non-calcified plaque burden (middle panel in red) on CT angiography, significant ^{18}F-NaF uptake and experienced a lateral non-ST-segment elevation myocardial infarction during follow-up.

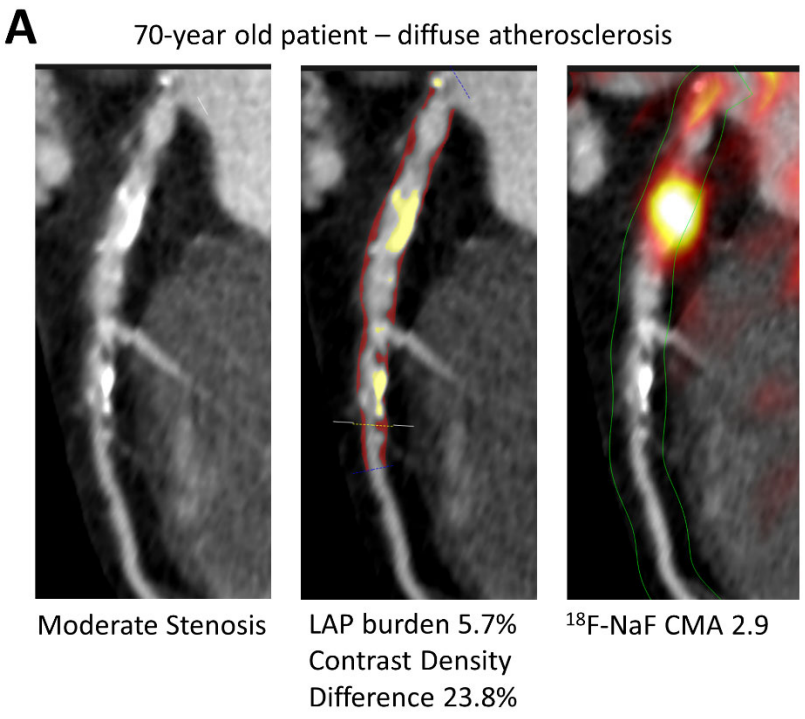

CMA – coronary microcalcification activity, LAD – left anterior descending, LCX – left circumflex, LAP – low attenuation plaque

Figure 3. Prediction of myocardial infarction by machine-learning. A) Receiver operator curves for the risk of myocardial infarction: ^{18}F-sodium fluoride (^{18}F-NaF) coronary microcalcification activity (CMA) alone (dark blue), machine learning models based on clinical data (light blue), quantitative plaque analysis (gray), clinical + quantitative plaque analysis + ^{18}F-NaF PET (red). The model based on both PET and quantitative CT-based plaque analysis data outperformed the clinical data and both unimodality models ($p<0.01$ for all). (B) Feature importance for the machine-learning model based on all variables. The solid bars and error bars represent the mean gain and standard deviation derived from the distribution of the importance within 10 folds of the cross testing, for each variable.

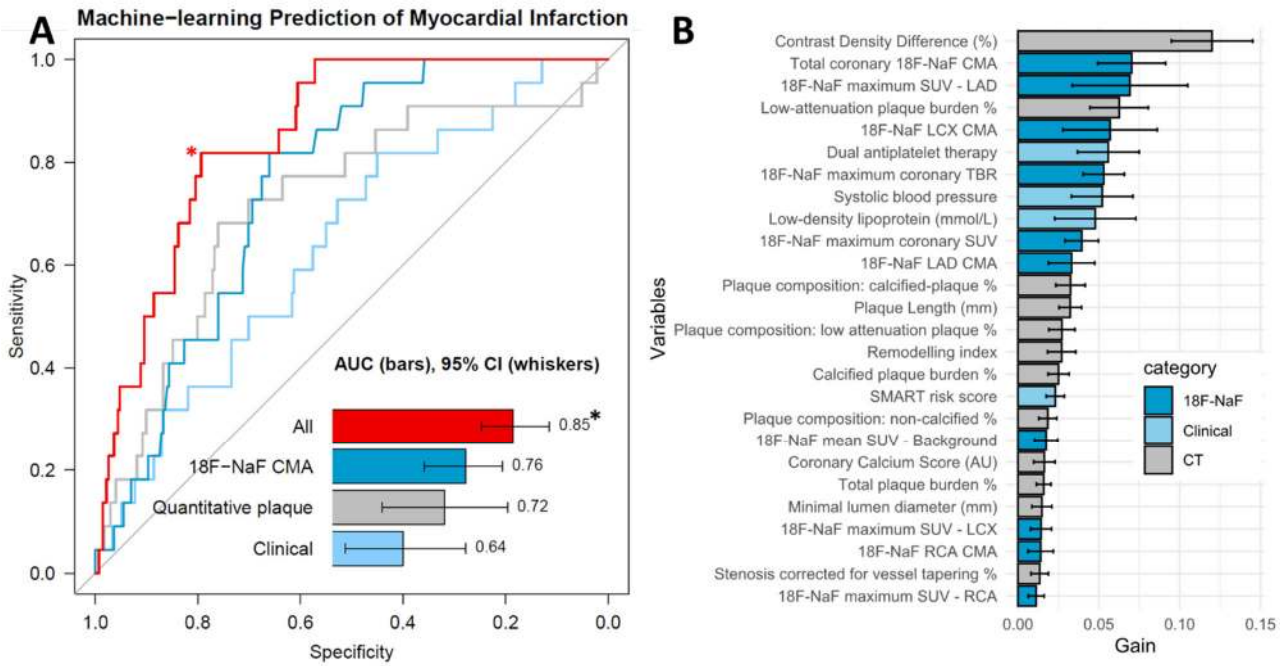

*indicates a $p<0.01$ for a difference compared to ^{18}F-NAF CMA, quantitative plaque, Clinical and CT (DeLong test)

#error bars indicate 95% confidence intervals

CMA – coronary microcalcification activity, SUV – standard uptake value, TBR – target to background ratio

Figure 4. Calibration plot for the clinical + quantitative plaque analysis + ^{18}F-NaF PET machine-learning XGBoost model. The calibration plot shows the relationship between the observed and predicted proportion of events, grouped by decile of risk. Our model showed very good calibration with the observed risk of myocardial infarction during follow-up.

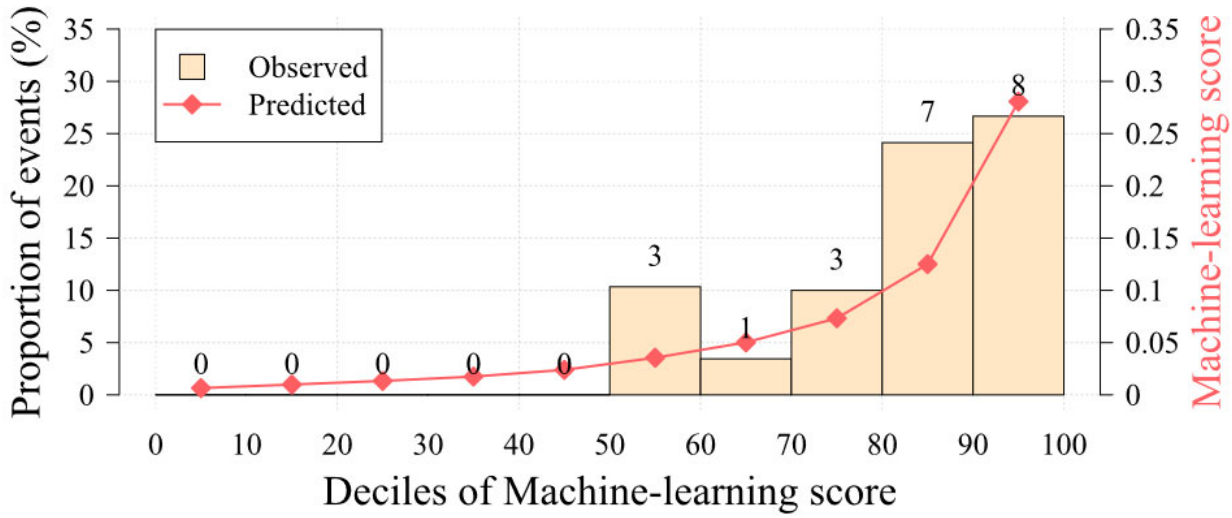

Supplementary Data

Machine-learning with ^{18}F-sodium fluoride PET and quantitative plaque analysis on CT angiography for the future risk of myocardial infarction

Jacek Kwiecinski[a,b], Evangelos Tzolos [a,c], Mohammed N Meah[c], Sebastien Cadet[a], Philip D Adamson[d], Kajetan Grodecki[a], Nikhil V Joshi [e], Michelle C Williams[c], Edwin JR van Beek MD, PhD [c,f], Daniel S Berman[a], David E Newby[c], Damini Dey[a], Marc R Dweck[c], Piotr J Slomka[a]

[a] Department of Imaging (Division of Nuclear Medicine), Medicine (Division of Artificial Intelligence in Medicine), and Biomedical Sciences, Cedars-Sinai Medical Center, Los Angeles, CA, USA
[b] Department of Interventional Cardiology and Angiology, Institute of Cardiology, Warsaw, Poland
[c] BHF Centre for Cardiovascular Science, University of Edinburgh, Edinburgh, United Kingdom
[d] Christchurch Heart Institute, University of Otago, Christchurch, New Zealand
[e] Bristol Heart Institute, University of Bristol, United Kingdom
[f] Edinburgh Imaging, Queens Medical Research Institute, University of Edinburgh, Edinburgh, United Kingdom

Methods

SMART score. The SMART (Second manifestations of arterial disease) risk score estimates the 10-year risk for myocardial infarction, stroke or vascular death in individual patients with previous cardiovascular disease, including coronary artery disease, cerebrovascular disease, peripheral artery disease, abdominal aortic aneurysm and polyvascular disease. The SMART risk score was developed in a population of vascular patients in the Netherlands that were included in the Secondary Manifestations of Arterial Disease (SMART)-study (1). External validation and updating were performed in pooled trial cohorts of 18,436 vascular patients from W-Europe, S-Europe, Israel, USA, Canada, Mexico, S-Africa, Australia, and N-Zealand (2). The SMART score calculators can be found at: https://www.escardio.org/Education/ESC-Prevention-of-CVD-Programme/Risk-assessment/SMART-Risk-Score

^{18}F-Sodium Fluoride PET

Image reconstruction

The ECG-gated PET list mode dataset was reconstructed using a standard ordered expectation maximization algorithm with time-of-flight, and point-spread-function correction. Using 4 cardiac gates, we reconstructed the data on a 256x256 matrix (with 75 or 47 slices using 2 iterations, 21 subsets and 5-mm Gaussian smoothing for Siemens mCT data and 4 iterations, 24 subsets and 5-mm gaussian smoothing for GE Discovery data) (3). To compensate for coronary motion associated with heart contraction, we performed cardiac motion correction of the PET/CT images as described previously (4). After motion-correction, the 4 images aligned to the end diastolic gated position were summed back together to build a motion-free image containing counts from the entire duration of PET acquisition. To offset for variation in the delay between

tracer injection and the PET acquisition, we employed a recently validated correction factor to harmonize the background activity to a reference 60-min injection-to-acquisition interval (5).

Coronary Microcalcification Activity

We used a recently described measure of coronary ^{18}F-NaF uptake, coronary microcalcification activity (CMA) that quantifies PET activity across the entire coronary vasculature (6). We automatically extracted whole-vessel tubular and tortuous 3D volumes of interest which encompass all the main epicardial coronary vessels and their immediate surroundings (4-mm radius) from CT angiography datasets (Figure 1). Within such volumes of interest, we measured CMA, representing the overall disease activity in the vessel and based upon both the volume and intensity of ^{18}F-NaF PET activity within it. CMA was defined as the integrated activity in standardized uptake value (SUV) exceeding the corrected background blood-pool mean SUV + 2 standard deviations. Since CMA is based on SUV (SUV=Pixel Value (Bq/ml)) * Weight(kg) / Dose (Bq) * 1000 (g/kg), and can be considered as: SUV units x volume, the CMA unit would be g/mL x mL = g. However, given the fact that in the equation the unitless measure of activity (derived from: Pixel Bq/ml/ Dose (Bq) plays a key role to avoid confusion we refrained from reporting CMA in grams.

We measured the background activity in the right atrium, drawing cylindrical volumes of interest (10-mm radius and 5-mm thickness) at the level of the right coronary artery ostium. The per-patient CMA was defined as the sum of the per-vessel CMA values. We calculated the per vessel and per patient maximum coronary SUV and target to background ratio (TBR) as described previously (7). In brief within 3 dimensional volumes of interest which encompassed coronary arteries the maximum standard uptake value (SUVmax) was recorded. TBR was calculated by dividing SUVmax by averaged background blood pool activity.

Machine-learning

The hyperparameters used for the XGBoost model were as follows:

Booster = gbtree

Learning rate = 0.005

Maximum depth of a tree = 1

Subsample ratio of the training instances = 0.6

Minimum sum of instance weight (hessian) needed in a child = 1

balance of positive and negative weights = 1

number of iterations = 5.000

10-fold repeated hold-out testing

The advantages of the 10-fold repeated hold-out testing over single split-sample approach are well documented and include: (1) reduction of variance in prediction error leading to a more accurate estimate of model performance; (2) maximizing the data for both training and validation, without overfitting or overlap between test and validation data; and (3) avoiding testing hypotheses suggested by arbitrarily split data (type III errors) (8,9).

Supplementary Table 1. Variables used in machine-learning.

Category	No.	Variable name
Clinical	1	abnormal rest ECG (0, 1)
	2	age (years)
	3	body mass index (kg/m^2)
	4	conduction disease (0, 1)
	5	current smoker (0, 1)
	6	past smoker (0, 1)
	7	diabetes mellitus (0, 1)
	8	dyslipidemia (0, 1)
	9	family history of premature coronary artery disease (0, 1)
	10	height (cm)
	11	hypertension (0, 1)
	12	past cerebrovascular accident
	13	past coronary artery bypass surgery (0, 1)
	14	past myocardial infarction (0, 1)
	15	past open-heart surgery (0, 1)
	16	past percutaneous coronary intervention (0, 1)*

17	peripheral vascular disease (0, 1)
18	coronary stent (0, 1)
19	coronary stent in LM, LAD
20	coronary stent in LCX
21	coronary stent in RCA
22	rest DBP (mmHg)
23	rest heart rate (bpm)
24	rest SBP (mmHg)
25	sex (m, f)
26	atrial fibrillation (0, 1)
27	weight (kg)
28	Aspirin (0, 1)
29	PY12_anatagonist (0, 1)
30	Statin (0, 1)
31	ACE inhibitors (0, 1)
32	ARB (0, 1)
33	Diuretic (0, 1)

34	Beta_Blocker (0, 1)
35	Calcium_Channel_Blocker (0, 1)
36	Isosorbide mononitrate (0, 1)
37	Nicorandil (0, 1)
38	Ivabradine (0, 1)
39	Warfarin/NOACS (0, 1)
40	Nitrate Spray (0, 1)
41	Metformin (0, 1)
42	Gliclazide (0, 1)
43	insulin (0, 1)
44	Proton pump inhibitors (0, 1)
45	Alpha blockers (0, 1)
46	Haemoglobin g/L
47	WBC n/dL
48	Platelets n/dL
49	Urea mmol/L
50	Sodium mmol/L

	51	Potassium mmol/L
	52	Creatinine mmol/L
	53	eGFR ml/m2
	54	Random Glucose mg/dL
	55	HbA1c %
	56	hsTnI ng/L
	57	Total Cholesterol mmol/L
	58	LDL mmol/L
	59	HDL mmol/L
	60	Triglycerides mmol/L
	61	SMART risk score (integer)
	62	Recent acute coronary syndrome (0, 1)*
Computed Tomography – qualitative and non-contrast	63	Duke coronary artery disease score (integer)
	64	Left Main Stenosis (0-5)
	65	pLAD Stenosis (0-5)
	66	mLAD Stenosis (0-5)
	67	dLAD Stenosis (0-5)

	68	Diagonal Stenosis (0-5)
	69	pLCx Stenosis (0-5)
	70	AVCx Stenosis (0-5)
	71	dLCx Stenosis (0-5)
	72	OM Stenosis (0-5)
	73	pRCA Stenosis (0-5)
	74	mRCA Stenosis (0-5)
	75	dRCA Stenosis (0-5)
	76	PDA Stenosis (0-5)
	77	Multivessel Disease (0, 1)
	78	Maximum Stenosis Grade (0-5)
	79	Obstructive coronary artery disease (0, 1)
	80	Segment Involvement Score (0-16)
	81	Coronary calcium score (integer)
	82	Coronary calcium score <1000 (0, 1)
	83	Coronary calcium score <1199 (0, 1)
	84	Total plaque volume (continuous)

Computed tomography - qualitative	85	Non-calcified plaque volume (continuous)
	86	Calcified plaque volume (continuous)
	87	Low attenuation plaque volume (continuous)
	88	Total plaque burden (continuous)
	89	Non-calcified plaque burden (continuous)
	90	Calcified plaque burden (continuous)
	91	Low attenuation plaque burden (continuous)
	92	Area stenosis (continuous)
	93	Contrast density difference (continuous)
	94	Minimal lumen area (continuous)
	95	Minimal lumen dimension (continuous)
	96	Remodelling index (continuous)
	97	Plaque length (continuous)
	98	Plaque composition LAP% (continuous)
	99	Plaque composition non-calcified plaque (continuous)
	100	Plaque composition calcified plaque (continuous)
	101	Ischemia score (continuous)

^{18}F-NaF	102	CMA (continuous)
	103	CMA LAD (continuous)
	104	CMA RCA (continuous)
	105	CMA LCX (continuous)
	106	CMA > 1.56 (0, 1)
	107	CMA < 0 (0, 1)
	108	Maximum TBR (continuous)
	109	Maximum SUV (continuous)

ACS – acute coronary syndrome, CMA – coronary microcalcificatin activity, CCS – coronary calcium score, CVA – cardiovascular accident, DG – diagonal, eGFR – estimated glomerular filtration rate, HDL – High density lipoprotein, LAD – left anterior descending, LCX – left circumflex, LMN – left main, LDL – low density lipoprotein, RCA – right coronary artery, SD – standard deviation, SIS – segment involvement score, SUV – standard uptake value, TAG – Triglicerydes, TBR – target to background ratio

*Because 61 patients in our study were subjects imaged shortly after an acute coronary syndrome for machine-learning we choose to differentiate them from subjects who had a percutaneous coronary intervention performed at a greater interval from PET imaging. These 61 patients were coded as recent ACS individuals and were considered positive for PCI only if an intervention was also conducted irrespective of the recent ACS.

References:

1. Dorresteijn JA, Visseren FL, Wassink AM, et al. Development and validation of a prediction rule for recurrent vascular events based on a cohort study of patients with arterial disease: the SMART risk score. Heart. 2013;99(12):866-72.

2. Kaasenbrood L, Boekholdt SM, van der Graaf Y, et al. Distribution of Estimated 10-Year Risk of Recurrent Vascular Events and Residual Risk in a Secondary Prevention Population. Circulation. 2016;134(19):1419-1429.

3. Doris MK, Otaki Y, Krishnan SK, Kwiecinski J, Dey D, Slomka PJ. Optimization of reconstruction and quantification of motion-corrected coronary PET-CT. J Nucl Cardiol 2020;27(2):494-504. doi: 10.1007/s12350-018-1317-5

4. Rubeaux M, Joshi N, Dweck MR, Dey D, Slomka PJ. Motion correction of 18F-sodium fluoride PET for imaging coronary atherosclerotic plaques. J Nucl Med 2016;57:54-9

5. Lassen ML, Kwiecinski J, Dey D, Newby DE, Dweck MR, Berman DS, Slomka PJ. Triple-gated motion and blood pool clearance corrections improve reproducibility of coronary 18F-NaF PET. Eur J Nucl Med Mol Imaging. 2019;46:2610–2620

6. Kwiecinski J, Cadet S, Dey D, Slomka PJ. Whole-vessel coronary 18F-sodium fluoride PET for assessment of the global coronary microcalcification burden. Eur J Nucl Med Mol Imaging. 2020;47:1736–1745

7. Joshi NV, Vesey AT, Williams MC, Dweck MR, Newby DE. 18F-fluoride positron emission tomography for identification of ruptured and high-risk coronary atherosclerotic plaques: a prospective clinical trial. Lancet 2014;383:705-13

8. Molinaro AM, Simon R, Pfeiffer RM. Prediction error estimation: a comparison of resampling methods. Bioinformatics 2005;21(15):3301-7.

9. Kohavi R. A Study of Cross-Validation and Bootstrap for Accuracy Estimation and Model Selection. IJCAI'95: Proceedings of the 14th international joint conference on Artificial intelligence; 1995, 1137-43.